Available online at www.sciencedirect.com

ScienceDirect

Ceramics International 40 (2014) 3989–3993

CERAMICS INTERNATIONAL

www.elsevier.com/locate/ceramint

Effects of liquid phases on densification of TiO_2-doped Al_2O_3–ZrO_2 composite ceramics

Yufei Zu, Guoqing Chen*, Xuesong Fu, Keguang Luo, Chunguang Wang, Shiping Song, Wenlong Zhou

School of Materials Science and Engineering, Dalian University of Technology, Dalian 116085, PR China

Received 24 June 2013; received in revised form 31 July 2013; accepted 9 August 2013
Available online 16 August 2013

Abstract

This study investigated the densification behaviors and microstructural evolution of Al_2O_3–ZrO_2 (3Y) composite ceramics doped with four different amounts of TiO_2 (0, 1, 4, and 8 wt%; denoted as 0T, 1T, 4T, and 8T, respectively) to clarify the effect of TiO_2 dopants on densification. The shrinkage rate during densification increased with the increase in the amount of TiO_2. The development of grain boundary feature was also examined. The undoped ceramic showed clean grain boundaries. Thin liquid grain boundary phases were observed in 1T, whereas large liquid phases were found on the grain boundary and at the junction pockets in 4T and 8T. The results were discussed in terms of the relationship between densification and grain boundary feature.

Keywords: Al_2O_3–ZrO_2 (3Y) ceramics; TiO_2 dopants; Densification enhancement; Grain boundary feature; Liquid phases

1. Introduction

Al_2O_3–ZrO_2 (3Y) composite ceramic is a structural material with wide applications. Given the excellent ambient and high-temperature mechanical properties of this material, it is mainly used as cutting tools, bearings, high-temperature engine components, and knee replacement prostheses. However, the sintering process requires very high temperatures. Thus, a key issue in the industrial application of structural ceramics is the reduction of sintering temperature to save production cost. To this end, several attempts to reduce sintering temperature have been made by using dopants. Akin et al. [1] added TiO_2 in Al_2O_3–ZrO_2 ceramic and observed a reduction in sintering temperature of about 150 °C. Huang et al. [2] investigated the sintering behavior of TiO_2-doped Al_2O_3–ZrO_2 ceramic. They found that TiO_2 dopants lower sintering temperature, and that levels of grain growth and hardness reduction are acceptable.

Although sintering enhancement through the addition of dopants is widely accepted, the enhancement mechanism remains unclear. Sintering enhancement of ceramic doped with cations is very complicated. Sintering rate may be affected by the diffusion improvement via excess vacancy, the transition of grain boundary features, the chemical bonding state of grain boundary, the second phase occurrence, and other factors. Many researchers have studied the effects of the addition of dopants during the sintering process. Brook and his co-workers [3–5] investigated the microstructural evolution during sintering and the optimization of the process and microstructures through the use of additives. Their classic works have provided an easy and convenient way to visualize a complex sintering problem. Dillon and Harmer [6,7] recently proposed a new concept of grain boundary feature called 'complexion' to study the relationship between the grain boundary diffusivity and grain boundary feature. In their previous studies [6–10], they found that the mass transport rate generally increases with increasing grain boundary disorder, grain boundary width, or grain boundary free volume. The concept is effective in guiding field researchers in appreciating the complexity of the sintering problem. Yoshida and his co-workers [11,12] investigated the ionic bonding state of TiO_2 doped in ZrO_2 and proposed that Ti dopants enhance the diffusion of Zr cations. Other aliovalent dopants in solid solution have been known to increase defect concentrations and hence the diffusivity.

*Corresponding author. Tel.: +86 411 84707970; fax: +86 411 84709967.
E-mail address: gqchen@dlut.edu.cn (G. Chen).

0272-8842/$ - see front matter © 2013 Elsevier Ltd and Techna Group S.r.l. All rights reserved.
http://dx.doi.org/10.1016/j.ceramint.2013.08.049

Bagley and Johnson [13] found that Ti^{4+} can promote alumina sintering through the formation and dissociation of dopant-defect complexes on lattice diffusivities. But Fielitz and his co-workers studied the ^{26}Al tracer diffusion in nominally undoped and Ti-doped single crystalline Al_2O_3 and found that Ti doping has little effect on lattice diffusion in Al_2O_3 in the recent papers [14,15]. Thus far, a clear enhancement mechanism for the sintering process in all ceramics has not been established.

TiO_2-doped Al_2O_3–ZrO_2 (3Y) composite ceramic has excellent mechanical properties and good densification ability. However, the mechanism for the densification enhancement of this material has yet to be investigated and thus remains unclear. The present study examines the densification behaviors and microstructural evolution of Al_2O_3–ZrO_2 (3Y) ceramics doped with different amounts of TiO_2 to clarify the effect of TiO_2 dopants on densification.

2. Experimental materials and methods

Nano-sized powders of the Al_2O_3–ZrO_2 (3Y) composite were prepared by the heating ethanol–aqueous salt solutions method [16]. The TiO_2 (Rutile) used in this study had purity of over 99.8%. Different amounts of TiO_2 (0, 1, 4, and 8 wt%; denoted as 0T, 1T, 4T, and 8T, respectively) were added to the as-calcinated Al_2O_3–ZrO_2 (3Y) powders by electromagnetic stirring and ultrasonic wave shaking.

TiO_2-doped Al_2O_3–ZrO_2 (3Y) composite powders were pressed uniaxially in a cylindrical die under ambient temperature. The cylindrical die was made of high-strength graphite and had a diameter of 10 mm. The preforms were then sintered by spark plasma sintering (SPS-3.20MK-IV, Sumitomo Coal Mining Co., Ltd., Japan) under 65 MPa at 1400 °C with a dwelling time of 6 min in vacuum. The temperature of these ceramics during sintering was measured by an infrared radiation thermometer. The sintering characteristic parameters, including temperature, pressure, and instantaneous specimen height, were recorded by the SPS system.

The shrinkage proceeded unidirectionally for each measured specimen. Assuming unidirectional shrinkage to compact powder, the density $\rho(T)$ at a given temperature T is given by the following equation:

$$\rho(T) = \frac{H_f}{H(T)}\rho_f, \quad (1)$$

where H_f and $H(T)$ are the final height and the height at temperature T, respectively. The final density ρ_f was measured by the Archimedes method. The density $\rho(T)$ at temperature T was calculated using Eq. (1).

Analysis of phase composites was performed by X-ray diffraction (XRD-6000, Shimadzu corporation, Japan). The microstructure was characterized by scanning electron microscopy (SEM S-4300, Hitachi, Japan). The SEM specimens were polished with 1.5 μm diamond paste and then thermally etched in air for 1 h at a temperature that was 50 °C lower than the sintering temperature. The average grain sizes of the two phases were calculated using the linear intercept method: $d = 1.56L$, where L is the intercept length. The grain boundary feature was characterized using a transmission electron microscope (TEM, TecnaiG220, FEI, the Netherlands).

3. Results and discussion

3.1. Powder preparation of TiO_2-doped Al_2O_3/ZrO_2 (3Y) composite

Nano-sized powders of Al_2O_3–ZrO_2 (3Y) composite were prepared by the heating ethanol–aqueous salt solutions method [16]. The Al_2O_3–ZrO_2 (3Y) powders were synthesized at a mass ratio of 58:42. The powders were then calcinated in air at 1100 °C for 2 h. The as-calcinated powders showed good dispersion, uniform grain size, and no hard agglomeration (Fig. 1a). The average particle size ranged from 20 nm to 30 nm, and the specific surface area was 20.3 $m^2\,g^{-1}$. The mass fraction of various components, including impurities in the Al_2O_3–ZrO_2 (3Y) composite powders, is shown in Table 1.

Rutile TiO_2 was added in as-calcinated Al_2O_3–ZrO_2 (3Y) powders by electromagnetic stirring and ultrasonic wave shaking. The TiO_2 used in this study had $>99.8\%$ purity. The average particle size of the TiO_2 powders was approximately 80 nm (Fig. 1b). The amount of TiO_2 additions were 0, 1, 4, and 8 wt%.

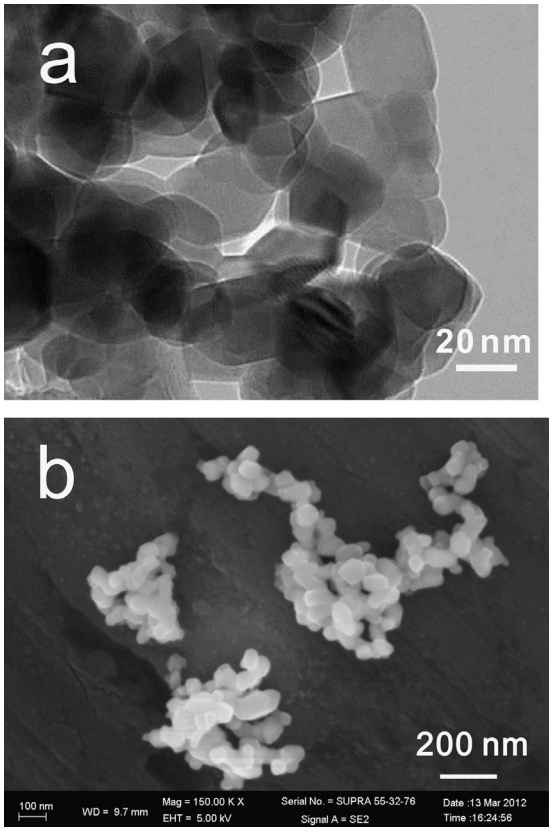

Fig. 1. TEM morphology of Al_2O_3–ZrO_2 (3Y) nano-sized powders (a) and SEM morphology of TiO_2 powders (b).

3.2. Densification behavior and microstructural analysis

Al_2O_3–ZrO_2 (3Y) doped with four different amounts of TiO_2 were sintered at 1400 °C with a dwelling time of 6 min. The shrinkage curves during the sintering process are shown in Fig. 2a. The sintering shrinkages of the four ceramics all began at ~1000 °C. However, the samples shrank at a fast rate with the addition of a high amount of TiO_2 when the temperature reached over 1100 °C. Using the shrinkage data, the dependence of relative density (ρ) on temperature (Fig. 2b) was calculated by Eq. (1). Fig. 2b shows that densification is enhanced by the addition of TiO_2. The ceramic becomes fully dense (> 99%) in 8T, 4T, and 1T at 1320 °C, 1370 °C, and 1400 °C, respectively. The relative density of the undoped ceramic is only 97.5% after dwelling time.

Fig. 3 shows the microstructures (at the surface parallel to the stress axis) of Al_2O_3–ZrO_2 (3Y) ceramics doped with four different amounts of TiO_2 sintered at 1400 °C. Al_2O_3 (dark) and ZrO_2 (white) grains are dispersed, and grain growth occurs by doping with TiO_2 additives. Some large liquid phases (50 nm to 100 nm thick) are observed along the edge facets and at the junction pockets in 8 T (marked by hollow arrows). This finding indicates that liquid phases exist on the grain boundary and thus affect the sintering process.

Table 1
Chemical composition of undoped Al_2O_3–ZrO_2 (3Y) ceramic.

Composition	Al_2O_3	ZrO_2	HfO_2	Y_2O_3	SiO_2	Others[a]
Mass fraction (%)	57.6	39.1	0.6	2.3	0.19	≤0.2

[a]Impurities (less than 0.1 wt%).

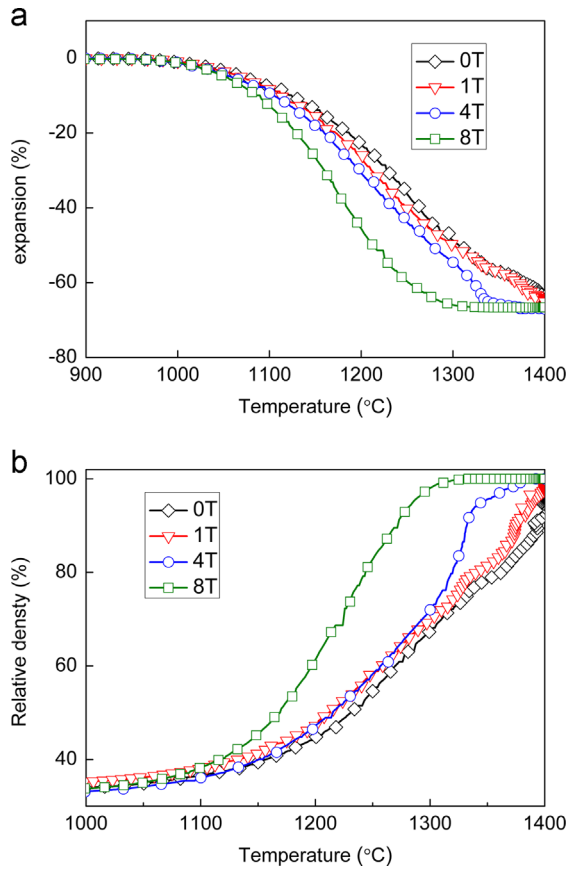

Fig. 2. Temperature dependence of expansion and relative density of 0T to 8T.

The typical XRD patterns of as-sintered 0T to 8T specimens are shown in Fig. 4. All the specimens show two phases, namely, α-Al_2O_3 and t-ZrO_2 (3Y). The SEM micrographs reveal the presence of some liquid phases in 8 T. However, no peak of TiO_2, $TiZrO_4$, or Al_2TiO_5 phase can be observed, as shown in the XRD pattern. The contradiction may be caused by the low sensitivity in XRD detection ($\geq$ 5 vol% is detectable).

3.3. Effect of liquid phase

The sintering results indicate that densification is enhanced by the addition of TiO_2. The densification improvement in doped ceramics may be affected by several factors, such as diffusion enhancement via excess vacancy [17,18], structure/chemistry of grain boundary [14,15], chemical bonding state of grain boundary [12,19], and second phase occurrence. Given the low limited solubility of TiO_2 in Al_2O_3 (~0.27 wt%) [20], a few Ti cations are dissolved in Al_2O_3 lattice. In some previous studies, it is confirmed that cation vacancy defects are generated due to the different valence between Ti^{4+} and Al^{3+} [17,18]. In the solid solution of Ti–Al_2O_3 lattice, one Ti cation substitute at Al site, while 1/3 Al vacancy defect [V'''_{Al}] formed. The Al ion vacancy defects may compose a path which Al ion can diffuse through rapidly in Al_2O_3 lattice. But Fielitz and his co-workers [14,15] reported that Ti doping has little effect on lattice diffusion in Al_2O_3 in the recent papers. For the doped ceramics (1T, 4T, and 8T) in this paper, the solubilities of Ti ions in Al_2O_3 lattice are the same. However, the densification is enhanced significantly by doping with more TiO_2 additions. Therefore, the enhancement of densification is not mainly caused by the excess vacancies in Al_2O_3. Due to its high limited solubility in ZrO_2 (~16 wt%) [21], and the distribution tendency of dopants, some Ti cations are dissolved in ZrO_2, while others segregate on grain boundaries. Yoshida et al. [12,19] studied the chemical bonding state of the grain boundary of ZrO_2 doped with Ti cation. They found that Ti cations reduce the ionicity between O anions (neighboring Ti cation) and Zr cations. The weakened ionic bonds can enhance the diffusion of Zr cations. Meanwhile, Ti cations segregated on grain boundaries change the grain boundary feature. Fig. 5a shows clean grain boundaries in the undoped composite ceramic. After doping the ceramic with TiO_2, the grain boundary feature changes. Several thin liquid grain boundary phases (1 nm to 2 nm thick) in 1T can be observed (Fig. 5b) at all types of interface, namely Al_2O_3–Al_2O_3, ZrO_2–ZrO_2, Al_2O_3–ZrO_2. Generally, the transition of grain boundary feature should affect the grain boundary transport rate and consequently the densification process. The distinction of these grain boundary features can be expressed by the difference of the width of the solute disordered cation layers on the grain boundaries (the width of the liquid grain boundary phase). The mass transport rate on grain boundary can increase with increasing the width of the grain boundary phase [6–10].

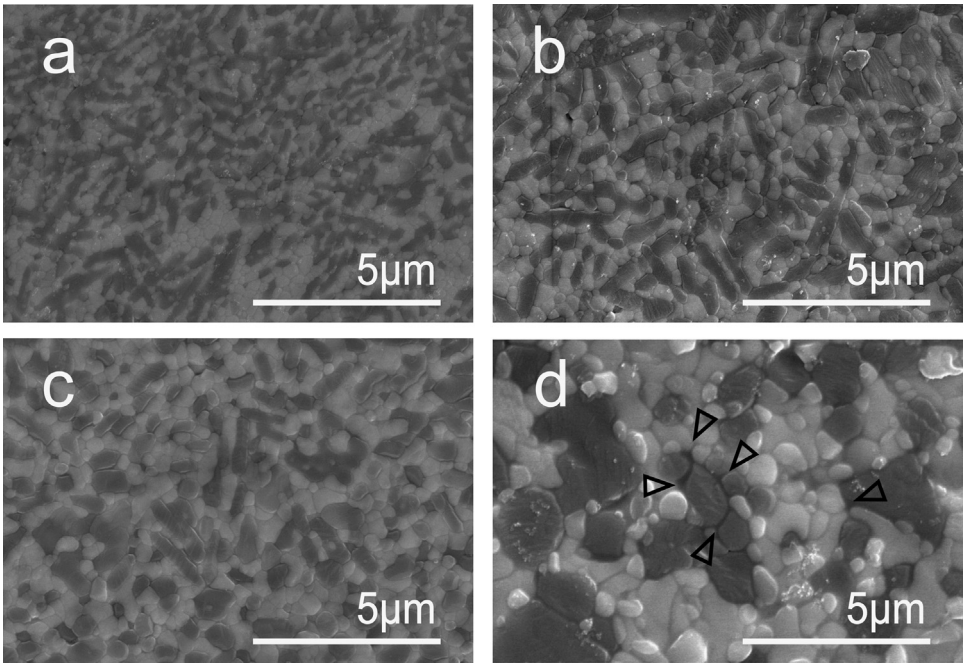

Fig. 3. Scanning electron microscopy images of (a) 0T, (b) 1T, (c) 4T, and (d) 8T sintered at 1400 °C by SPS. The dwelling time at sintering temperature is 6 min. The specimens were polished and thermally etched in air for 2 h at 1350 °C.

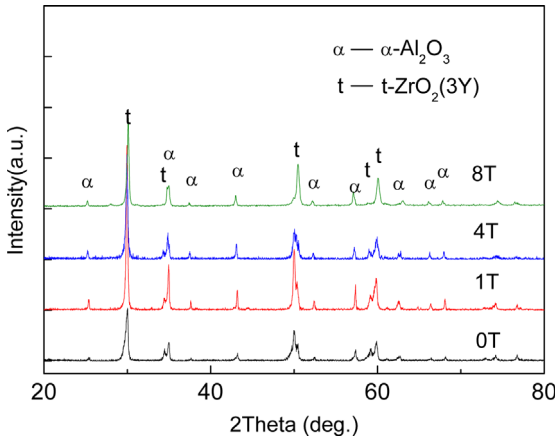

Fig. 4. XRD patterns of Al_2O_3–ZrO_2 (3Y) ceramics: undoped, 1T, 4T, and 8T.

In 1T, there are a lot of intergranular films with equilibrium thickness (1 nm to 2 nm thick) on grain boundaries. By contrast, the undoped ceramic showed clean grain boundaries. Therefore, the movement of the atoms at the grain boundary is enhanced by the transition of the interface structures. Consequently, the densification of the 1 wt% TiO_2-doped ceramic is improved mainly by the weakened Zr–O ionic bonds and by the occurrence of the thin grain boundary liquid phases.

The concentrations of Ti cations dissolved in the ZrO_2 grains and segregated on the grain boundaries in 4T and 8T are higher than those in 1T. The increase of Ti cations in ZrO_2 improves the diffusion in ZrO_2 during sintering. However, diffusion enhancement due to weakened ionic bonds in 4T and 8T may not be sufficient to significantly improve densification. Notably, some large liquid phases (Fig. 5c) can be observed on the grain boundary and at the junction pockets in 4T and 8T. The liquid phase should enhance densification because of its viscous flow ability during the final sintering process, high cation diffusion via liquid phase, high grain boundary migration, and its ability to eliminate cavities. The liquid phases in 8T (detected by TEM and SEM) are larger and greater in number than those in 4T (detected only by TEM). This condition indicates that sintering enhancement by large liquid phases in 8T is more significant than that in 4T. In summary, densification enhancements in 4T and 8T are dominated by the occurrence of large liquid phases.

4. Conclusion

The densification behaviors and microstructural evolution of Al_2O_3–ZrO_2 composite ceramic doped with four different amounts of TiO_2 were investigated. Densification is enhanced significantly by TiO_2 doping. After TiO_2 doping, Ti cations reduce the ionicity of the Zr–O bond; thus, the Zr cations can move easily. Furthermore, grain boundary feature changes with TiO_2 concentration. Most of grain boundaries are clean in the undoped ceramic. By contrast, thin grain boundary liquid phases appearing in 1T and large liquid phases appearing in 4T and 8T can be detected in the TiO_2-doped Al_2O_3–ZrO_2 ceramic. Given the microstructure features and densification behaviors observed in the study, the densification enhancement in 1T is attributable to the weakened ionic bonds and the thin grain boundary liquid phases; in 4T and 8T, the densification enhancement is attributable to the occurrence of large liquid phases.

Acknowledgments

This work was supported by the National Natural Science Foundation of China nos. 50875032, 51175059, and 50505005,

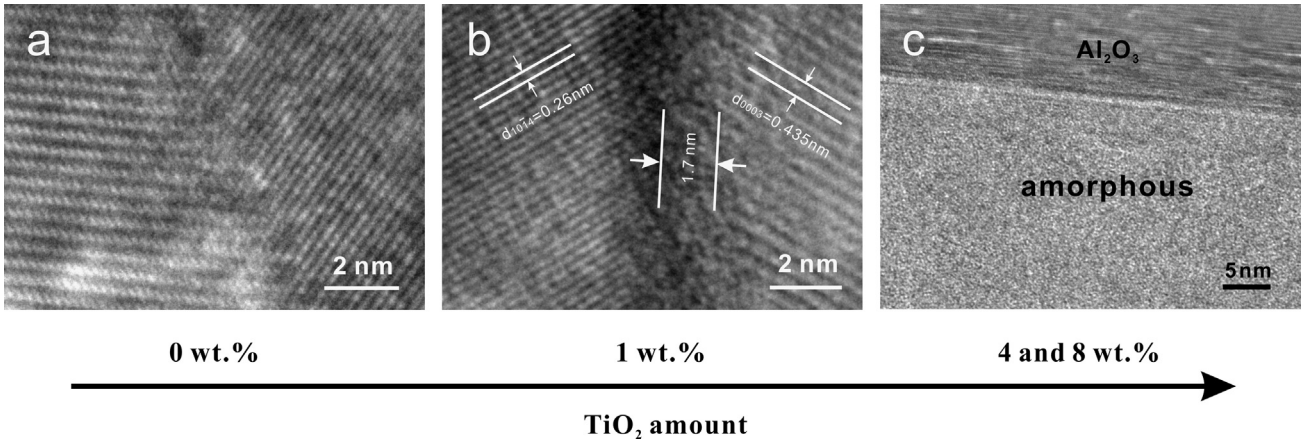

Fig. 5. Different grain boundary features in the undoped and doped ceramics: low level grain boundary complexion (a) before TiO_2 doping, thin grain boundary liquid phase (b), and the large liquid phase (c) after TiO_2 doping.

and by the Program for New Century Excellent Talents in University under Grant no. NCET-10-0278.

References

[1] I. Akin, E. Yilmaz, O. Ormanci, F. Sahin, O. Yucel, G. Goller, Effect of TiO_2 addition on the properties of Al_2O_3–ZrO_2 composites prepared by spark plasma sintering, Bioceramics Development and Applications 1 (2011) 1–3.

[2] C.J. Wang, C.Y. Huang, Effect of TiO_2 addition on the sintering behavior, hardness and fracture toughness of an ultrafine alumina, Materials Science and Engineering 492 (1–2) (2008) 306–310.

[3] R.J. Brook, Additives and the sintering of ceramics, Science of Sintering 20 (2–3) (1988) 115–118.

[4] L.A. Xue, Y. Chen, E. Gilbart, R.J. Brook, The kinetics of hot-pressing for undoped and donor-doped $BaTiO_3$ ceramics, Journal of Materials Science 25 (2) (1990) 1423–1428.

[5] R.J. Brook, Effect of TiO_2 on the initial sintering of Al_2O_3, Journal of the American Ceramic Society 55 (2) (1972) 114–115.

[6] S.J. Dillon, M. Tang, W.C. Carter, M.P. Harmer, Complexion: a new concept for kinetic engineering in materials science, Acta Materialia 55 (18) (2007) 6208–6218.

[7] S.J. Dillon, M.P. Harmer, Multiple grain boundary transitions in ceramics: a case study of alumina, Acta Materialia 55 (15) (2007) 5247–5254.

[8] S.J. Dillon, M.P. Harmer, G.S. Rohrer, Influence of interface energies on solute partitioning mechanisms in doped aluminas, Acta Materialia 58 (15) (2010) 5097–5108.

[9] S.J. Dillon, M.P. Harmer, Demystifying the role of sintering additives with complexion, Journal of European Ceramic Society 28 (7) (2008) 1485–1493.

[10] S.J. Dillon, S.K. Behera, M.P. Harmer, An experimentally quantifiable solute drag factor, Acta Materialia 56 (6) (2008) 1374–1379.

[11] H. Yoshida, A. Kuwabara, T. Yamamoto, Y. Ikuhara, T. Sakuma, High temperature plastic flow and grain boundary chemistry in oxide ceramics, Journal of Materials Science 40 (12) (2005) 3129–3135.

[12] H. Yoshida, K. Morita, K. B-N, H. K, Ionic conductivity of tetragonal ZrO_2 polycrystal doped with TiO_2 and GeO_2, Journal of the European Ceramic Society 29 (2009) 411–418.

[13] R.D. Bagley, I.B. Cutler, D.L. Johnson, Effect of TiO_2 on initial sintering of Al_2O_3, Journal of the American Ceramic Society 53 (3) (1970) 136–141.

[14] P. Fielitz, G. Borchardt, S. Ganschow, R. Bertram, A. Markwitz, ^{26}Al tracer diffusion in titanium doped single crystalline α-Al_2O_3, Solid State Ionics 179 (11–12) (2008) 373–379.

[15] P. Fielitz, G. Borchardt, S. Ganschow, R. Bertram, ^{26}Al tracer diffusion in nominally undoped single crystalline a-Al_2O_3, Defect and Diffusion Forum 323–325 (2012) 75–79.

[16] G.Q. Chen, K.F. Zhang, G.F. Wang, L. Zhang, Preparation and characterization of nano-sized Al_2O_3/ZrO_2 powders, Materials Science & Technology 12 (2004) 20–23.

[17] A.M. Anthony, Sintering and related phenomena materials science research, vol. 6[M], Plenum Press, New York, 1973.

[18] D.M. Smyth, The defect chemistry of metal oxides, Extrinsic Ionic Disorder, Vol. 5, Oxford University Press72–73.

[19] H. Yoshida, Y. Ikuhara, T. Sakuma, Grain boundary electronic structure related to the hightemperature creep resistance in polycrystalline Al_2O_3, Acta Materialia 50 (11) (2002) 2955–2966.

[20] Y.M. Kim, S.H. Hong, D.Y. Kim, Anisotropic abnormal grain growth in TiO_2/SiO_2-doped alumina, J. Am. Ceram. Soc. 83 (11) (2000) 2809–2812.

[21] T. Noguchi, M. Mizuno, The solubility limit of TiO_2 in the pure ZrO_2, Bulletin of the Chemical Society of Japan 41 (1968).